Elsevier Editorial System(tm) for Energy and Buildings
Manuscript Draft

Manuscript Number:

Title: CFD analysis of heat collection in a glazed gallery

Article Type: Full Length Article

Keywords: Glazed gallery; CFD; Energy-efficient building; Solar passive design.

Corresponding Author: Mrs. María José Suárez López, Chemical Engineer

Corresponding Author's Institution: University of Oviedo

First Author: María José Suárez López, Chemical Engineer

Order of Authors: María José Suárez López, Chemical Engineer; Antonio J Gutiérrez, Ph. D. ; Jorge Pistono, Ph. D.; Eduardo Blanco, Ph. D.

Abstract: A glazed gallery in most old buildings is used both as a space to insulate the adjacent rooms and as a leisure area, among other applications. In the framework of the ARFRISOL project (Bioclimatic Architecture and Solar Cooling), a demonstration container has been built in northern Spain (Asturias) which includes, among other bioclimatic elements, a glazed gallery that enables solar radiation to be collected and the energy obtained to be used to support the building's air conditioning system. It consists of a south-facing glazed exterior wall, an intermediate space or passage and a partially-glazed interior wall. Dampers located in the floor and ceiling of the intermediate space and connected to the air ducts enable the air circulating inside the gallery to be heated or cooled, depending on the season of the year, before it is further conditioned and conveyed to the rooms. This paper focuses on the three-dimensional numerical simulation of the airflow inside the gallery. The aim is to obtain a model to evaluate the thermal energy obtained in this architectural feature, integrating the effect of certain variables, such as the incident solar irradiation, the outdoor temperature and the air flow rate circulating in the gallery.

Cover Letter

Dear Sirs

The ARFRISOL project (Bioclimatic Architecture and Solar Cooling) aim is to demonstrate the feasibility of bioclimatic systems and absorptive solar air conditioning in real buildings. One of these systems is the glazed gallery, which has been the object of the research presented in this article.

In this case, the gallery has been designed not only as insulation, but to be part of the conditioning system, by the collection of the sun warmed air. The numerical analysis done shows the heat power available and the influence of the solar radiation and external temperature. Some comparisons have been made with experimental data and, also, a brief study of the economic aspects.

We hope you find the article interesting and worthy of publication in the Journal.

Yours sincerely

María José Suárez López

CFD analysis of heat collection in a glazed gallery

María José Suárez[*], *Antonio José Gutiérrez, Jorge Pistono, Eduardo Blanco*

Universidad de Oviedo, EDZE (Energía), Campus de Viesques, 33271 Gijón (Asturias) Spain.

[*]Corresponding author. Tel.: +34 985182366.
E-mail address: suarezlmaria@uniovi.es (M.J. Suárez).

Abstract

A glazed gallery in most old buildings is a space located on the first floor (and/or higher floors), facing south and almost fully glazed. As a result of the large glazed area and the orientation of the gallery, its temperature is warmer than the exterior and, in cold weather, it is used both as a space to insulate the adjacent rooms and as a leisure area, among other applications. In the framework of the ARFRISOL project (Bioclimatic Architecture and Solar Cooling), a demonstration container has been constructed in northern Spain (Asturias) which includes, among other bioclimatic elements, a glazed gallery. This gallery is considered as an element of bioclimatic architecture that enables solar radiation to be collected and the energy obtained to be used to support the building's air conditioning system. It consists of a south-facing glazed exterior wall, an intermediate space or passage and a partially-glazed interior wall. Dampers located in the floor and ceiling of the intermediate space and connected to the air ducts enable the air circulating inside the gallery to be heated or cooled, depending on the season of the year, before it is further conditioned and conveyed to the rooms. This paper focuses on the three-dimensional numerical simulation of the airflow inside the gallery. The aim is to obtain a model to evaluate the thermal energy obtained in this architectural feature, integrating the effect of certain variables, such as the incident solar irradiation, the outdoor temperature and the air flow rate circulating in the gallery.

Keywords: Glazed gallery, CFD, Energy-efficient building, Solar passive design.

1. Introduction

The aim of Bioclimatic Architecture is to achieve an adequate level of hygrothermal comfort by adapting the design, geometry, orientation and construction of the building to the environmental conditions of its surroundings. It involves an architecture adapted to the environment, sensitive to the impact it causes on nature, and designed to minimise energy consumption –and, consequently, environmental pollution– by making use of the available natural resources (sun, vegetation, rain, wind, etc.). This type of architecture is used, above all, to achieve passive air conditioning systems that are integrated in the structure of the building, either as basic structural items (walls, windows, roofs, etc.), or as basic items with a modified function (greenhouses, galleries, chimneys, basements, etc.). A detailed description of these and other items can be found in [1].

The development of Bioclimatic Architecture, and the passive and active use of solar energy as the most appropriate energy source for environmental conditioning in buildings, led to the launch and promotion in Spain of a Singular Strategic Project, called Bioclimatic Architecture and Solar Cooling (ARFRISOL). The aim of the project is to study the energy behaviour of several demonstration containers (new or renovated) located in five different environmental conditions. The intention is to demonstrate that the use of bioclimatic structural elements (glazed galleries, greenhouses, shading devices, ventilated roofs, etc.) and renewable energies (biomass, solar energy, geothermal energy, etc.) can help reduce both final energy consumption and carbon dioxide emissions to the atmosphere [2]. This paper presents a study of the bioclimatic aspect of a glazed gallery in the demonstration container located in the north of Spain.

A conventional gallery is a space similar to a closed-in balcony, but generally larger in size. It is typically found in single-family dwellings, on the first floor (and/or higher floors) and has no thermal contact with the ground. It consists of a south-facing glazed exterior wall, an intermediate space –used as a leisure area, play area for young children, as a place to dry clothes, etc.– and a partially-glazed wall separating the gallery from the adjacent room (Fig. 1). It has always been recognized, even before it had ever been analysed in detail, that this sun warmed area helps, to some extent, in the heating of the adjacent rooms.

In Bioclimatic Architecture, the gallery is strictly defined as a building solution consisting of a south-facing glazed exterior wall, an intermediate space for passage and a partially-glazed interior wall separating the gallery from the adjacent rooms. There are some differences between this solution and the Trombe wall or the greenhouse, which are also widely used in bioclimatic buildings. On the one hand, the width of the intermediate space in this solution is considerably greater than in the case of a Trombe wall, but smaller than in a greenhouse. Furthermore, in the greenhouse and gallery the interior partition wall is partially glazed, whereas in the case of the Trombe wall it is usually completely opaque. This glazed portion allows solar irradiation to pass directly into the adjacent rooms. The main difference between the gallery and the greenhouse lies in the width of the intermediate space. In the former, the space is so narrow that it serves for passage and little more, whereas in the latter it is large enough to be used as an extra room.

The gallery analysed in this paper is built in the demonstration container located in Asturias, northern Spain. Fig. 2 shows a photograph of the building, and Fig. 3 one of the interior of the gallery. Dampers are provided in the floor and ceiling of the intermediate space connecting the gallery to the outside air. There are also dampers at the lower side of the wall to the adjoining room and at the ceiling, connected to the air duct leading to the HVAC equipment (Fig. 4).

Depending on the position of the dampers, the gallery can be closed, connected to the exterior, or the air can be circulated through the gallery and to the HVAC equipment before it is conveyed to the adjacent rooms. The aim is to study the thermal behaviour of the gallery and investigate the possibility of supplementing the air conditioning system.

The operating principle changes depending on the position of the dampers. In winter conditions, the gallery allows both direct and diffuse solar radiation to be used, with two possible configurations: if all the dampers are closed, the gallery is used to insulate the adjacent rooms. On the other hand, if the louvers that connect to the adjacent rooms and the conditioning equipment are open and those to the exterior are closed, the energy collected in the gallery preheats the air (coming from the room) that circulates through it before it goes to the HVAC unit (Fig. 5 left). This reduces the amount of energy that the heating system has to provide in order to heat the air up to the required temperature.

In summer conditions, the gallery is rather a disadvantage as the air inside it is heated by the radiation received to a higher temperature than the outside, acting as a heat source rather than an insulation to the adjoining rooms. In this respect, the least disadvantageous configuration is the one in Fig. 5 right, where the louvers in the floor and ceiling are open and those to the rooms are kept closed. This configuration creates a draught in the gallery, which ventilates the space and prevents the air from stagnation, and consequently from heating up; it even could reduce the energy demanded by the HVAC system.

The problem now consists on the analysis of the thermal behaviour of the gallery and the best utilization of these possibilities.

Systematic research on this subject is relatively new because specific literature on glazed galleries and greenhouses attached to dwellings begins to appear in the 80s. For example Fuchs and McClelland [3] write about a “transwall” (a kind of little gallery), and Jones [4] includes them in his “Passive solar design handbook”. From the beginning there is a great interest in the performance determination of these solutions, looking for models to quantify the heat collection and transmission. Some of these analyses were accomplished with the help of simple numerical simulations [5, 6], and others use the experimental technique, mainly searching to validate the numerical models [7, 8].

As mentioned previously, a glazed gallery partly operates in a similar way to a Trombe wall, which is a widely used system for which there is ample literature (descriptions, numerical analyses and experimental measurements), see for example references [9] to [12]. The main difference being that, in the Trombe solution, a wall of considerable mass accumulates the energy and releases it gradually to the inhabited premises. But it does not allow natural light to pass to the adjacent rooms, and there is no interior glazed partition except in special designs. Also, the separation between the exterior and interior walls is quite narrow, with a very small air volume.

There are also many articles that compare different bioclimatic construction elements (Trombe walls, transwalls and sunspaces) [13, 14] based on both experimental data and numerical simulations, to determine which offers the best performance. Although the analyses are not fully conclusive, many authors coincide in highlighting the superior performance of glazed spaces [3, 15, 16].

About numerical simulations of glazed spaces, it has been previously commented that some articles with very basic models appeared in the 80s. More detailed and precise models have appeared recently. The articles by Wall [17], Cardinale and Ruggiero [18], and Bakos [19], present comparative analyses of different software programmes, together with the results of simulations made with some of them, estimating the energy performance of the specific building solutions evaluated.

Finally, there are hardly any articles on the economic aspect of this subject and conclusions differ widely. For example, Bakos and Tsagas [20], state that the investment cost of a glazed space is recovered through energy savings in only a few months, whereas Tzipoulos [21] says that such structures did not provide any improvement in the energy efficiency of the buildings he analysed.

This article describes a numerical study of the movement of air inside the gallery in winter conditions, as the main purpose of the gallery is to take advantage of the solar radiation to reduce the amount of energy used in the heating of the building. The analysis takes into account both the solar irradiation on the glazed surface and its transmission to the adjacent rooms, either directly through the glazed areas or indirectly through the opaque surfaces heated by it. A general purpose computational fluid dynamics (CFD) software package (Fluent) valid for modelling three-dimensional flows was used. Satisfactory results were obtained that describe the thermal behaviour of the air flow developed inside the gallery, and quantify the energy collected in this bioclimatic solution for the conditioning of the adjacent rooms.

2. Methodology

The CFD (Computational Fluid Dynamics) code used solves the heat transfer and fluid dynamics problems simultaneously with the Navier-Stokes equations. Prior to the three-dimensional numerical analysis, tests were made with a simplified two-dimensional model to check the suitability of the boundary conditions selected. The results of these tests are detailed in [22].

Fig. 6 presents the 3D geometry solved. Symmetry was used at both sides to calculate only a portion of the gallery. The real geometry has five windows (and the corresponding dampers) matching five identical rooms. Any end effects were ignored and as compromise between the real geometry and the computational resources. The model is 1.88 m long, 3.90 m high and 0.97 m deep. The exterior glazing covers the whole front, the dimension of the interior window is 1.63x2.11 m and the louvers to the room and the conditioning equipment are 0.5x0.25 m. The dampers to the exterior have not been implemented because only the heat collection (winter) is going to be studied.

A structured mesh was used (Fig. 7), refined in some places such as the areas around the air inlet and outlet, and meshes were constructed for the solid materials (opaque and semitransparent) to calculate the conductive heat transfer through them. Some tests

were performed, varying the number of cells between 100000 and 2000000 to check the grid convergence and the turbulence models. Fig. 8 shows the heat flow per unit time collected from the air circulating through the gallery for the K-epsilon (RNG) and Reynolds Stress models (other models as the K-epsilon Standard and K-w have differences smaller than 5%). As it can be seen in the figure, beyond approximately 1 million cells, the variation in the results obtained with the different turbulence models is not very significant and, on the basis of the results, stability and calculation time, the K-epsilon (RNG) model were selected. Moreover, these equations provide good results, even if the system is rather laminar [23]. The complete calculations were performed with a mesh of 1050000 cells.

In the gallery, a large part of the heat transfer takes place by radiation. Following an exhaustive analysis of the available radiation models, the Discrete Ordinate method [24] were chosen because it allows radiation through semitransparent materials, such as glass, to be simulated. This model solves the heat radiation equation for a finite number of discrete solid angles (defined by the number of divisions and the number of pixels), each associated with a vector direction fixed in the global Cartesian system of coordinates. In order to achieve a compromise between the speed of the simulations, the computational resources, the size of the files and the accuracy of the results, a detailed study of the angular parameters was made, which led to the selection of 3 divisions and 16 pixels. This method also allows visible radiation to be differentiated from infrared radiation. To this end, the number of bands is defined –in this case 2– and each band is characterized by the wavelength interval (visible radiation waveband from 0.4 to 2.9 μm; infrared radiation waveband from 2.9 to 1000 μm) and by the radiation absorption coefficients for the semitransparent materials.

The fluid circulating in the gallery is air and ideal gas behaviour is assumed for the calculation of the density and to take into account the buoyancy effects. As regards the materials, the floor and the ceiling are made of composite (thickness: 0.05 m; thermal conductivity: 0.035 W/mK) and the opaque walls of limestone (thickness: 0.12 m; thermal conductivity: 2.25 W/mK). Behind there is a layer of insulation (thickness: 0.06 m; thermal conductivity: 0.04 W/mK) so that the heat transfer is negligible compared to the glazing. They are considered to be opaque materials to radiation and were assigned an emissivity value of 0.9 and a diffuse reflection value of 1%.

The exterior glazing of the gallery consists of a single-sheet of laminated glass (thickness: 0.01 m; thermal conductivity: 1.03 W/mK), whereas the interior wall has double glazing (6-10-5, 0.021 m) and an equivalent thermal conductivity of 0.119 W/mK calculated using the UNE-EN-673.

The glazing is semitransparent to radiation and two different absorption coefficients have been used for the two wavebands defined in the Discrete Ordinate model: 30 m^{-1} for the visible waveband and 450 m^{-1} for the infrared one. The refractive index for clear glass is approximately 1.52 [25].

The thermal boundary conditions assumed on the glazed surfaces, forming the contour of the domain analysed, allow the heat transmitted by convection and radiation to be taken into account. The convection heat transfer coefficients were defined as 23 $W/m^2 \cdot K$ for the outer side of the exterior glazing and 8 $W/m^2 \cdot K$ for the interior surface of the glazing in the partition wall (UNE-EN-673). Radiation was divided between direct and diffuse types. For the first type, the parameter used was solar radiation perpendicular to the exterior glazing, and for the diffuse radiation, the temperature of the source was defined as similar to the ambient temperature. Finally, 0.837 was taken as the emissivity value for both glazing on their respective surfaces facing outwards from the domain studied (UNE-EN-673).

The exterior air temperature was varied between 4 ºC and 14 ºC, a normal temperature range in winter conditions in northern Spain, while the indoor air temperature in the room was set to 20 ºC, slightly lower than the mean room temperature given in the current regulations for buildings in winter, because the room is a little colder near the window.

The radiation model selected allows the solar irradiation received on semitransparent materials to be directly defined. For the sake of simplicity, only the irradiation component perpendicular to the glazed surface was considered, with values between 100 and 800 W/m^2 with 100 W/m^2 intervals.

Finally, as regards the air inflow and outflow, it was assumed that the air enters the gallery from the room at 20 ºC and that the temperature of the outgoing air is one of the results obtained in the simulations. A constant velocity was used for the incoming air flow, while the outgoing airflow has a constant static pressure boundary condition. The air speed was varied between 0.132 and 2.64 m/s. These values cover a range of air flows going from 10% to 200% of the rated value of the HVAC equipment used to condition the rooms (600 m^3/h or 0.2 kg/s at 20 ºC).

About the factors that affect the accuracy of the results, second order discretization was applied for the equations and the convergence criterion was set so that the normalised value of all the residuals were lower than 10^{-6}.

3. Model analysis

In order to make a first qualitative analysis of the results, a scenario has been selected with an outdoor temperature of 8 ºC, solar irradiation of 600 W/m^2 and the nominal air mass flow rate (0.2 kg/s). Fig. 9 shows the temperature map and the velocity vectors in the cross-section of the gallery: it can be seen that the opaque materials (vertical walls, floor and ceiling) are warmer than the glass surfaces and that, of the two glazing areas, the outer one is colder because it limits with the exterior. The warmest area is the gallery ceiling, as it is the highest part and an area of stagnation –as can be seen in the velocity vectors in the plane of symmetry– but the main heating of the circulating air takes place at the inner vertical surface.

With respect to the air trajectory, the foregoing figure (9), and the more detailed Fig. 10, where the stream lines are plotted, show that the air comes out through the louver (located below the window), flows directly against the outer glass surface and back towards the inner one, forming a toroidal flow structure. Subsequently, the air flows parallel to the inner vertical wall and window, gets warmer as it rises towards the louver in the ceiling, and finally flows out through it to the HVAC unit.

Fig. 11 shows the temperatures at the interior of the gallery; the bottom part of the limestone inner wall is at a lower temperature because the air flow reaching it has received little heat (it has only come into contact with the outer glazed surface, which is the coldest part of the gallery). At it gets warmer it rises and comes into contact with the warmer part of the solid wall, which further increases the air temperature.

The glass of the interior window is colder than the opaque walls as not all the solar radiation received is absorbed, but most is transferred into the room and a smaller part is reflected again into the gallery. When the rising air comes into contact with the inner glazing, it continues to get warmer but the effect is less intense because the lower surface temperature, as commented above, and because only part of the absorbed radiation is transferred to the air in the gallery –the other part is conveyed to the room-.The same figure shows that there is an area of the opaque wall and the window, just above the louver, at a higher temperature than the rest. This effect is induced by the air stream entering the gallery, which blocks the ascending air, almost completely eliminating any flow parallel to the inner wall above the louver and reducing its cooling. The opposite effect takes place at the symmetry, equidistant from the inlet vents.

To corroborate the numerical results, some thermograms were taken of the interior and exterior of the gallery with an infrared camera, but it was not possible to make a good comparison because a global controlling system has not yet been implemented, and each room (there are five offices adjoining the gallery) has separate settings. Also, the difference in the materials emissivity makes the temperature interpretation rather problematic. Nevertheless, the thermograms are shown in Fig. 12 and an attempt at a qualitative examination has been made, taking into account that, at the time the images were obtained, the solar radiation perpendicular to the gallery was 380 W/m^2, the exterior temperature was 16 ºC, and that the temperatures measured inside the gallery, at 5 cm from the inner wall for floor, middle and ceiling height, were respectively 30, 38 and 47 ºC. The air in the gallery was relatively still because the recovery system was only partly active.

At the frontal thermogram (left), two bands with square pattern can be seen above and below the gallery glazing. These bands correspond to integrated photovoltaic modules, and they are hotter due to the heat rejected by the cells. These modules have not been implemented in the numerical model because they are not usually employed in glazed galleries; nevertheless, they are translucent and –leaving apart the small amount of electricity obtained- they tend to increase the heat collection due to the augmented absorptivity of the combined material. The exterior glazing has a temperature around 32 ºC, somewhat lower than the interior temperature. The lower part of the glazing is slightly hotter -in spite of the lower air temperature at that zone- owed to the higher infrared radiation of the limestone wall at the base of the inner surface; although this have not been shown, the same trend is observed in the simulations with very low flow. The interior limestone wall (bottom right) is rather hot, its mean temperature about 51 ºC. A colder spot can be appreciated, corresponding to a louver –not visible because it is recessed- connecting with a room (the air coming from the room is about 25 ºC). Some thin vertical lines are visible, generated by light reflected on a strut. The ceiling surface (upper right) has a temperature close to 41 ºC, not as hot as the limestone because it receives no direct radiation but it is heated by the ascending air. A closed damper can also be seen; it seems hotter than the rest of the ceiling, but the measurement is distorted by its higher emissivity.

These measurements approximate the results obtained in the simulations performed with the lower values of mass flow rate but, as stated previously, a precise comparison was not possible since the magnitude and distribution of the air flow could not be established.

Coming back to the numerical model, a parametric study of the heat collection has been made, and a quantitative analysis is presented in the following section.

4. Heat collection results

Several tests were performed with the numerical model varying the exterior temperature between 4 and 14 ºC, the perpendicular radiation between 100 and 800 W/m^2 and the mass flow rate between 0.01 and 0.4 kg/s. The results have been used to define the heat that can be collected in the gallery and the trends with the different variables.

Fig. 13 shows the heat transfer rate to the air flowing through the gallery versus the incident solar radiation perpendicular to the gallery glazing, keeping the nominal air mass flow rate constant and varying the outdoor temperature. It can be seen that the power collected for a given outdoor temperature increases linearly with the solar radiation. There is a minimum radiation value above which the energy can be collected from the exterior source. For example, with an outdoor temperature of 6 ºC (and a mass flow rate of 0.2 kg/s), if the solar radiation received is less than 300 W/m^2, the heat transfer is negative, i.e. the air would left the gallery cooler than at the inlet. This is contrary to the effect intended and, therefore, the use of the gallery with this configuration would be counterproductive. This minimum required irradiation value varies with the outdoor temperature: the higher the outdoor temperature, the smaller the amount of solar radiation needed. The gradient of the lines is practically the same in all cases, which means that as the radiation rises, the increment in the energy collected is independent of the outdoor temperature. With the nominal flow rate, the energy per unit time obtained in the gallery increases about 150 W for every 100 W/m^2 raise in solar radiation.

Fig. 14 shows the heat transfer rate to the air versus its mass flow rate for different solar radiations, at a constant outdoor temperature of 10 ºC (average value in winter conditions). As a rule, the energy collected increases as the air flow rises, but the trend is not linear. The increase is more marked at lower mass flow rates but, above a certain value, the increment is smaller and tends to stabilise. For example, with a radiation of 500 W/m^2, varying the mass flow rate from 0.01 to 0.2 kg/s, produces a considerable increase, from 125 W to 450 W, whereas if the previous flow rate is doubled (from 0.2 kg/s to 0.4 kg/s), the increment is only 75 W. With other solar radiation values, the tendency is basically the same.

In the figure it can also be seen that, as the radiation increases, the value of the air mass flow rate above which the heat transfer rate tends to stabilise increases as well. The opposite occurs with low values of solar radiation and, with 300 W/m^2, it even decreases a little. Moreover, with very low irradiation levels (lower than the values in the figure), and low outdoor temperatures - early in the morning, for example-, the use of the gallery to obtain energy could be counterproductive, as the energy losses are so high that the indoor air would get cooler instead of warmer.

To clearly illustrate this effect, Fig. 15 shows the heat transfer rate to the air through the gallery versus the solar radiation received for different flow rates, with a lower temperature than in the previous case (6 ºC). With solar radiation values above 400 W/m^2, the higher the mass flow rate, the more energy is collected, whereas with values of less than 400 W/m^2 this power is a little higher as the flow rate diminishes. Furthermore, the critical solar irradiation level above which energy begins to be obtained rises as the air flow rate increases.

Additionally, in this figure, it can be observed that, for the higher flow rates, the slope of the curve is quite linear (see also Fig. 13), while for the lower flow rate, the trend fluctuates a little. This phenomenon is linked with small changes in flow behaviour with when the air velocity is very low.

To summarise, as a general rule, the higher the level of solar radiation received, the greater the energy that can be collected in the gallery. With respect to the air mass flow rate, the power obtained grows with it, but the increase rate tends to diminish with high flow rates. Therefore, it is not worth to use very high flow rates, as this increases the power required to overcome the transport load losses, with only a slight increase in the heat power collected.

With the outdoor temperature happens the same as with the other two parameters studied: with higher outdoor temperatures more energy is obtained. This gain is mainly owed to lower heat losses through the gallery glazing.

Special care must be taken in the case of low irradiation, as the heat transfer may become inverted. For each outdoor temperature, there is a minimum solar radiation above which the energy can be collected in the gallery.

Finally, to make a brief analysis of the energy performance of the gallery, the heating requirements have been compared with the heat power that can be collected. Based on the building conditioning project, with an outdoor temperature of 6 ºC, the heating requirements per room are around 780 W, while with an outdoor temperature of 14 ºC, these requirements go down to around 340 W. The energy per unit time that can be collected with the nominal flow rate can be deduced from Fig. 13. It has to be taken into account that not all the heat power available can be employed; for example, when the level of irradiation is around 800 W/m^2 and the outdoor temperature is 14 ºC, approximately three times the amount of energy required for heating can be obtained, although the average values are usually much lower. The integration of the daily distribution of irradiation received during a sunny day with an average outdoor temperature of 6 ºC shows that the potential energy savings amount to 15%, while with an average outdoor temperature of 14 ºC the average savings could double, up to 32% of the heating requirements.

This demonstrates that a glazed corridor as described could be a substantial contribution to energy saving and, therefore, to environmental cleanliness. Nevertheless, coming down to monetary units, which cannot be forgotten, there are many factors to be considered, as the dimensions of the interior room and the gallery, its insulation and the price of the energy used. To give a comprehensive conclusion, a comparison has been made employing the customary building specifications for this location.

The cost of a normally build gallery has been offered by local contractor at around 700 €/m^2. The front of the room at Barredo is 3.9 m and the gallery width 1 m, giving an additional cost for the gallery of roughly 2750 € per room. If the gallery were not present, assuming good insulation, internal temperature of 20 ºC and external of 6 ºC, the average thermal load of a winter day is estimated between 800 and 1000 W. Electricity price is today 0.1177 €/kWh, this means between 2.3 and 2.8 € per winter day. With similar calculations for the typical spring and autumn days, the prospects are not gratifying: even if the glazed corridor would provide the whole heating energy, it would take around 5 years to pay back the gallery, and even this depends on money interest rate. Obviously, if the saving is around 25 % of the energy, nowadays the gallery cannot be justified by strictly economic reasons.

However, if a glazed corridor is considered for other purposes, as its use for leisure, aesthetics and so, in addition to the environmental preservation, the energy savings (in the climate analyzed) could contribute with 100 to 125 € per year (and room) to capital repayment.

5. Conclusions

This study adds to the existing body of knowledge about the thermal and fluid-dynamic behaviour of bioclimatic structures, more specifically of a glazed gallery, an intermediate case between the Trombe wall (extensively studied) and the attached greenhouse.

The results obtained show that its behaviour is intimately linked to the weather conditions (irradiation and outdoor temperature). Generally, the higher the irradiation and outdoor temperature values, the more energy can be collected in the gallery.

Another fundamental parameter in this study is the mass flow rate of air circulating inside the gallery. As a general rule, and as occurs with the parameters mentioned previously (irradiation and outdoor temperature), the thermal energy collected in the gallery increases as the flow rises, although energy collection does not increase linearly, and above a given flow rate value it tends to stabilise.

From an energy standpoint, the study demonstrates that a glazed gallery is a construction solution that can provide substantial savings. Specifically, with the weather conditions studied, on a clear winter day, between 15% and 32% of the energy required to heat the space next to the gallery could be obtained with this system.

These energy savings can help to cover the gallery costs, although the economic point of view cannot be the main reason for its building.

6. Acknowledgements

This work was carried out in the framework of the Singular Strategic Project ARFRISOL, on bioclimatic architecture and solar cooling (Reference: PS-120000-2005-1), funded by the Spanish Ministry of Education and Science (MEC) and co-funded by ERDF.

7. References

[1] Suárez, M.J., González, M., Aguilera, J.A., García, D., 2007. Los elementos bioclimáticos en el LIDER, Proceedings of CIATEA07, Congreso Internacional de Aislamiento Térmico y Acústico, Gijón, Asturias (Spain).

[2] Bosqued, A., Palero, S., San-Juan, C., Soutullo, S., Enríquez, R., Ferrer, J.A., Martí, J., Heras, J., Guzmán, J.D., Jiménez, M.J., Bosqued, R., Heras, M.R., 2006. ARFRISOL, bioclimatic architecture and solar cooling project, Proceedings of PLEA2006 Passive and Low Energy Architecture, Geneva (Switzerland).

[3] Fuchs, R., McClelland, J.F., 1979. Passive solar heating of buildings using a transwall structure. Solar Energy, 23, 123-128.

[4] Jones, R.W., 1981. Passive solar design handbook, DOE passive and hybrid solar energy program update conference, Washington, DC (USA).

[5] Jones, R.W., McFarland, R.D., 1980. Attached sunspace heating performance estimates, 5th National Passive Solar Conference, Amherst, Massachusetts (USA).

[6] Shoda, M.S., Nayak, J.K., Bansal, N.K., Goyal, I.C., 1982. Thermal performance of a solarium with renovable insulation. Building and Environment, 17, 23-32.

[7] McFarland, R., 1980. Performance estimates for attached sunspace passive solar heated buildings, Annual meeting of American section of the International Solar Energy Society, Phoenix, Arizona (USA).

[8] Shaviv, E., 1984. The performance of a passive solar house with window sunspace systems. Energy and Buildings, 7, 315-334.

[9] Gan, G., 1998. A parametric study of Trombe walls for passive cooling of buildings. Energy and Buildings, 27, 37-43.

[10] Torcellini, P., Pless, S., 2004. Trombe walls in low-energy buildings: practical experiences, World Renewable Energy Congress VIII, Denver, Colorado (USA).

[11] Chel, A., Nayak, J.K., Kaushikm, G., 2008. Energy conservation in honey storage building using Trombe wall. Energy and Buildings, 40, 1643-1650.

[12] Yilmaz, Z., Kundakci, A.B., 2008. An approach for energy conscious renovation of residential buildings in Istanbul by Trombe wall system. Building and Environment, 43, 508-517.

[13] Bakos, G.C., 2000. Energy management method for auxiliary energy saving in a passive-solar-heated residence using low-cost off-peak electricity. Energy and Buildings, 31, 237-241.

[14] Bakos, G.C., 2002. Improved energy management method for auxiliary electrical energy saving in a passive-solar-heated residence. Energy and Buildings, 34, 699-703.

[15] Nayak, J.K., 1987. Transwall versus Trombe wall: relative performance studies. Energy Conversion and Management, 27, 389-393.

[16] Fernández-González, A., 2007. Analysis of the thermal performance and comfort conditions produced by five different passive solar heating strategies in the United States Midwest. Solar Energy, 81, 581-593.

[17] Wall, M., 1997. Distribution of solar radiation in glazed spaces and adjacent buildings. A comparison of simulation programs. Energy and Buildings, 26, 129-135.

[18] Cardinale, N., Ruggiero, F., 2000. Energetic aspects of bioclimatic buildings in the Mediterranean area: a comparison between two different computation methods. Energy and Buildings, 31, 55-63.

[19] Bakos, G.C., 2003. Electrical energy saving in a passive-solar-heated residence using a direct gain attached sunspace. Energy and Buildings, 35, 147-151.

[20] Bakos, G.C., Tsagas, N.F., 2000. Technology, thermal analysis and economic evaluation of a sunspace located in northern Greece. Energy and Buildings, 31, 261-266.

[21] Tzikopoulos, A.F., Karatza, M.C., Paravantis, J.A., 2005. Modeling energy efficiency of bioclimatic buildings. Energy and Buildings, 37, 529-544.

[22] Suárez, M.J., Sarries, I., Pistono, J., 2008. Numerical analysis of the preheating performance of a glazed corridor in an office building, Proceedings of WREC08, World Renewable Energy Congress X and Exhibition, Glasgow (Scotland, United Kingdom).
[23] Chen, Q., 1995. Comparison of different K-epsilon models for indoor airflow computations. Numerical Heat Transfer, Part B: Fundamentals, 28, 353-369.
[24] Modest, M.F., 2003. Radiative heat transfer, second ed., Academic Press, California.
[25] Nicolau, V.P., Maluf, F.P., 2001. Determination of radiative properties of commercial glass, Proceedings of PLEA2001 Conference on Passive and Low Energy Architecture, Florinápolis (Brazil).

Figures

Fig. 1. Drawing of a traditional gallery.

Fig. 2. Photograph of demonstration container in northern Spain (South side). The gallery goes from the centre to the left.

Fig. 3. Interior of the glazed gallery.

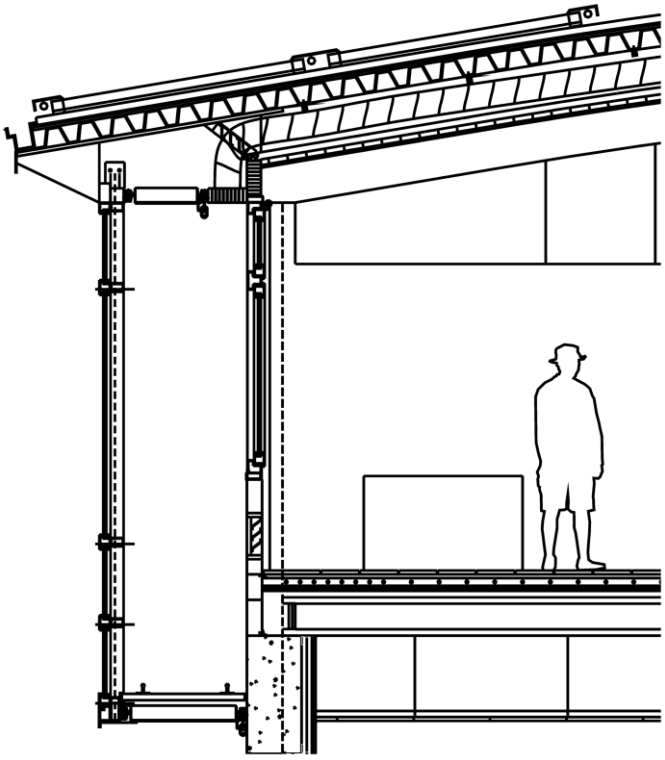

Fig. 4. Cross-section of the gallery and the adjoining room.

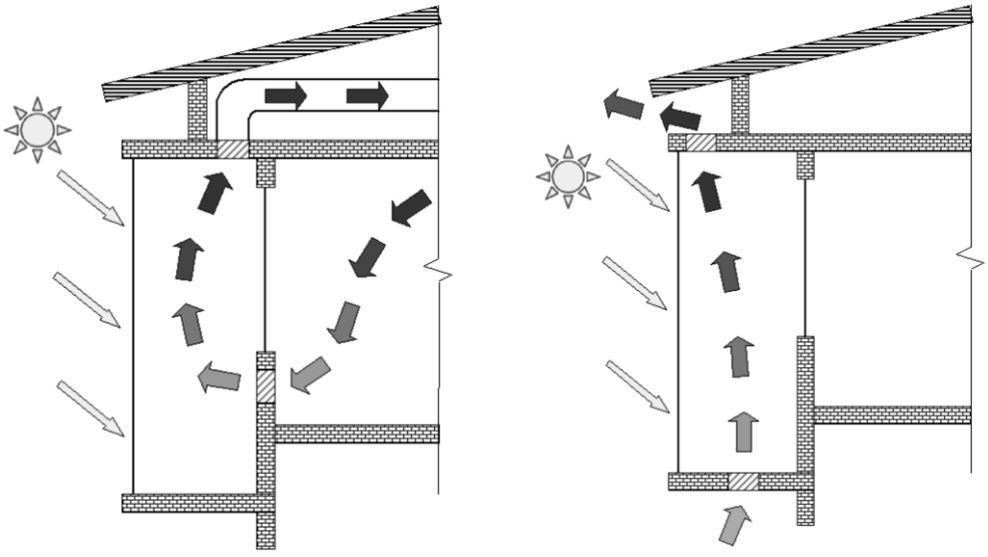

Fig. 5. Operation of the gallery in winter (left) and summer (right) conditions.

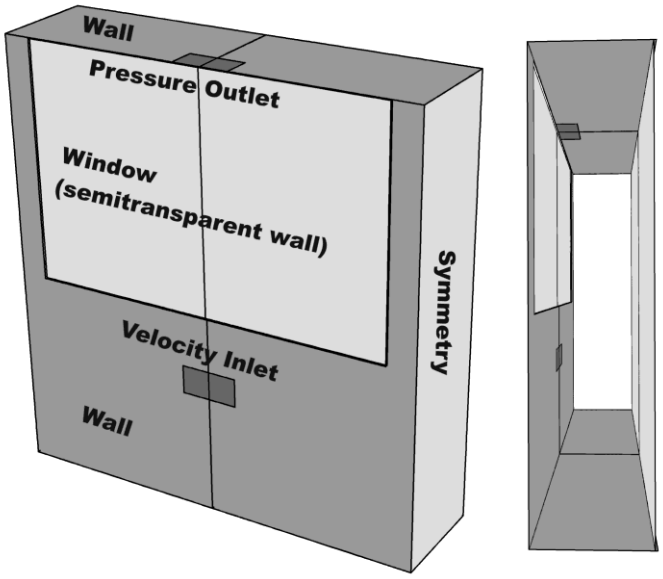

Fig. 6. Geometry and boundary conditions. View from inside the room and along the gallery.

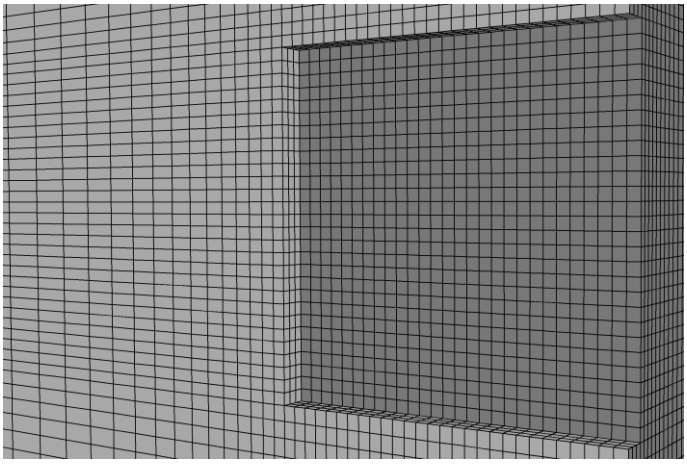

Fig. 7. Detail of the mesh at the inlet damper.

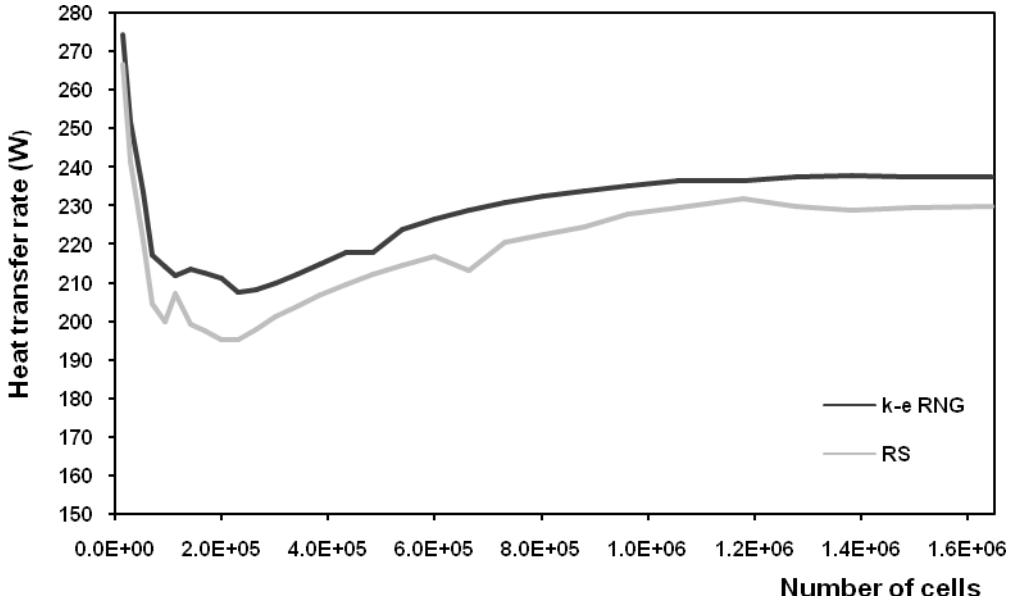

Fig. 8. Study of the turbulence model versus the number of cells.

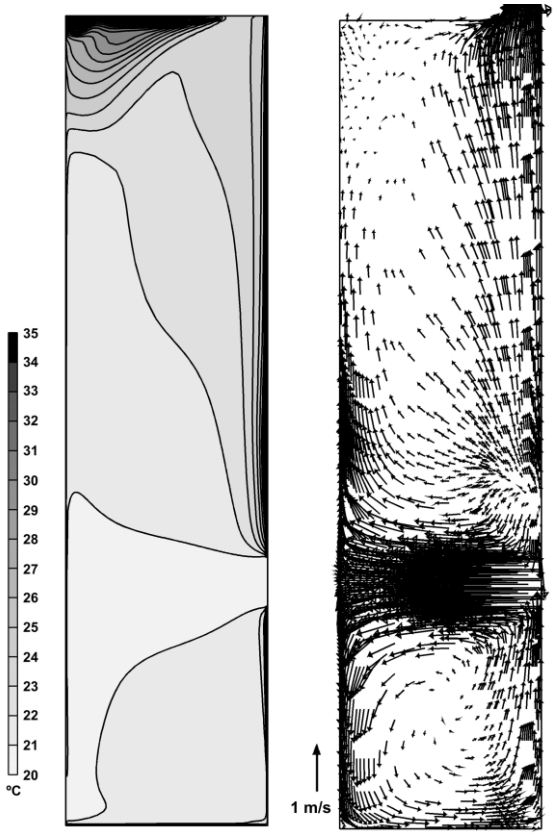

Fig. 9. Temperature contours and velocity vectors in the middle cross-section.

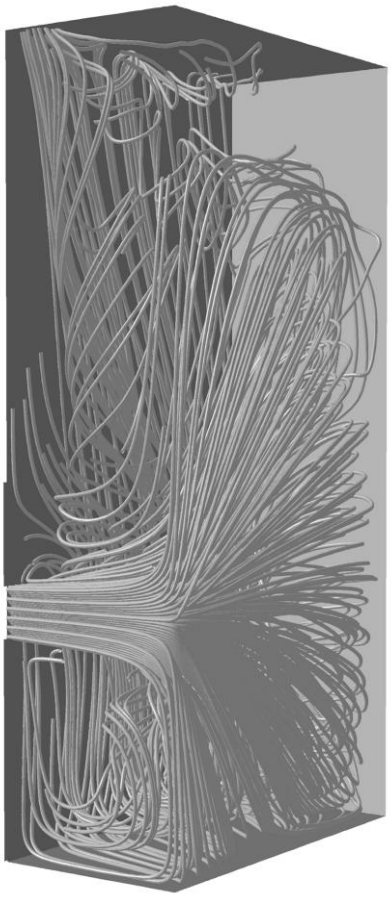

Fig. 10. Stream lines coming out from the inlet louver.

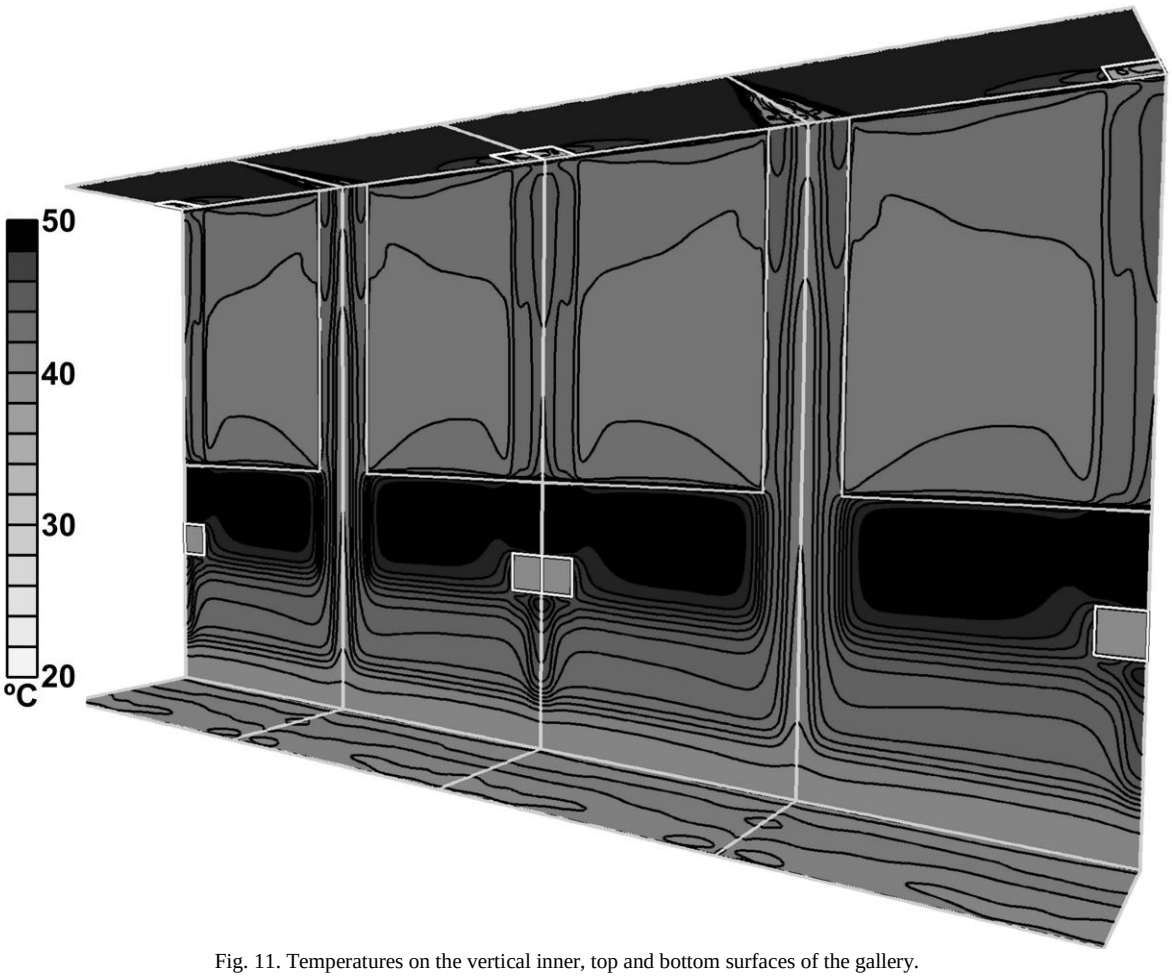

Fig. 11. Temperatures on the vertical inner, top and bottom surfaces of the gallery.

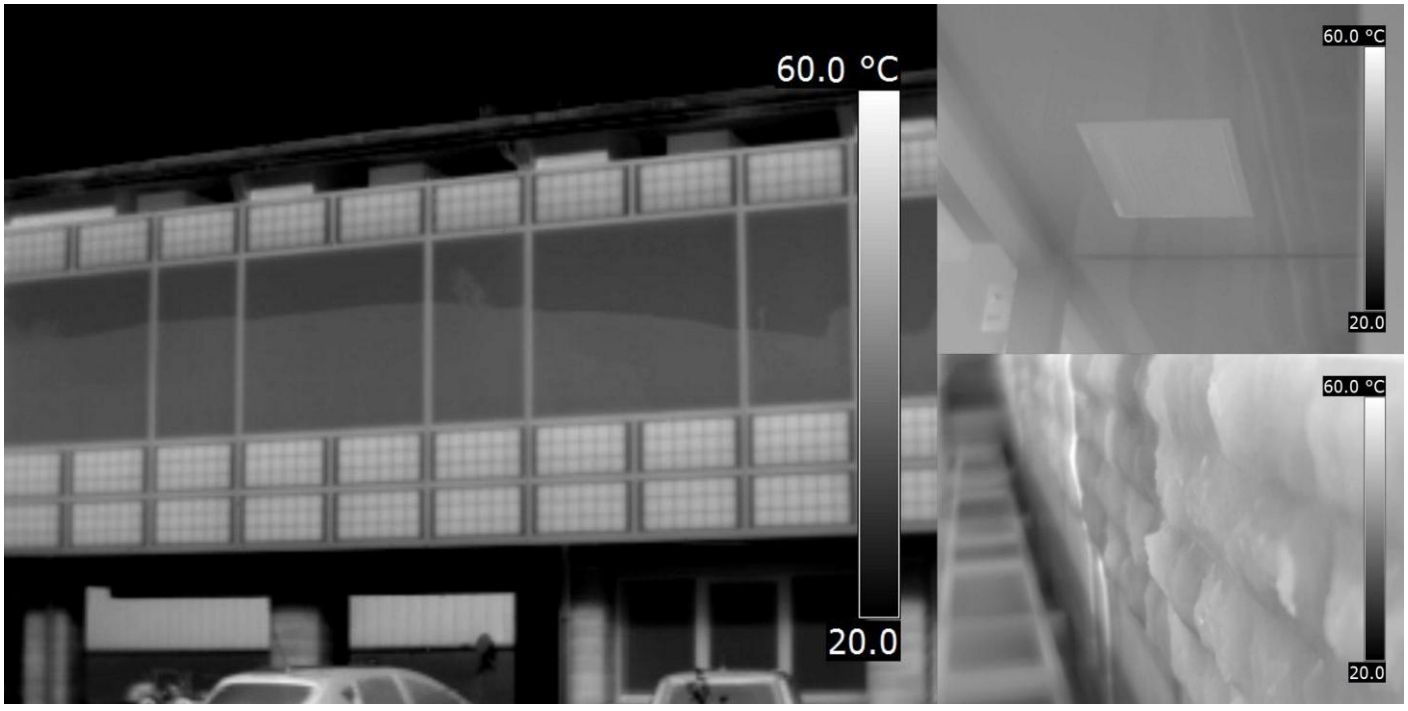

Fig. 12. Thermograms of the exterior and interior of the gallery (perpendicular solar radiation 380 W/m^2, exterior temperature 16 ºC).

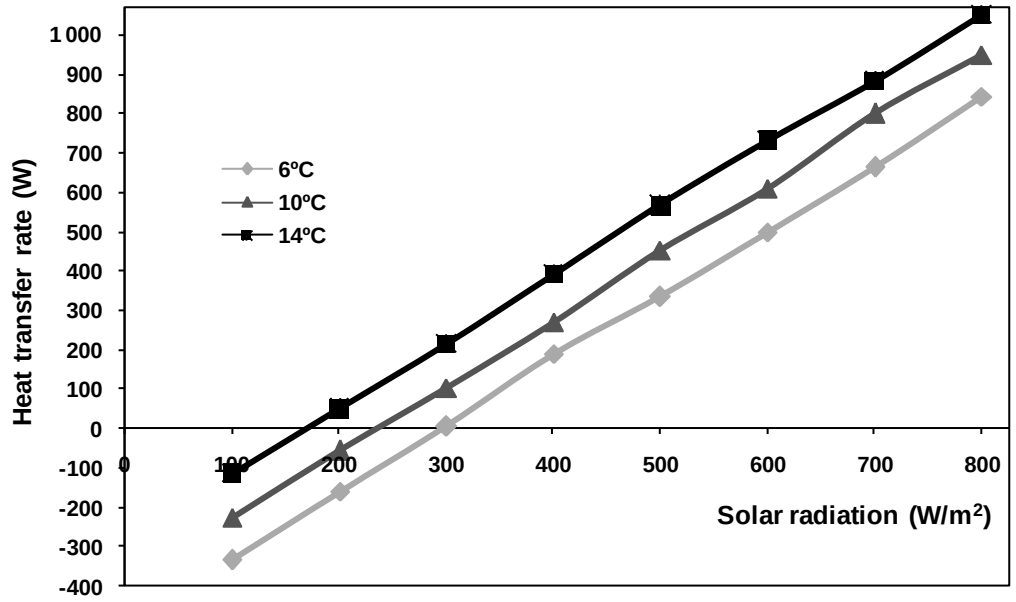

Fig. 13. Heat transfer rate to the air flow vs. perpendicular solar radiation, for different exterior temperatures (nominal mass flow rate 0.2 kg/s).

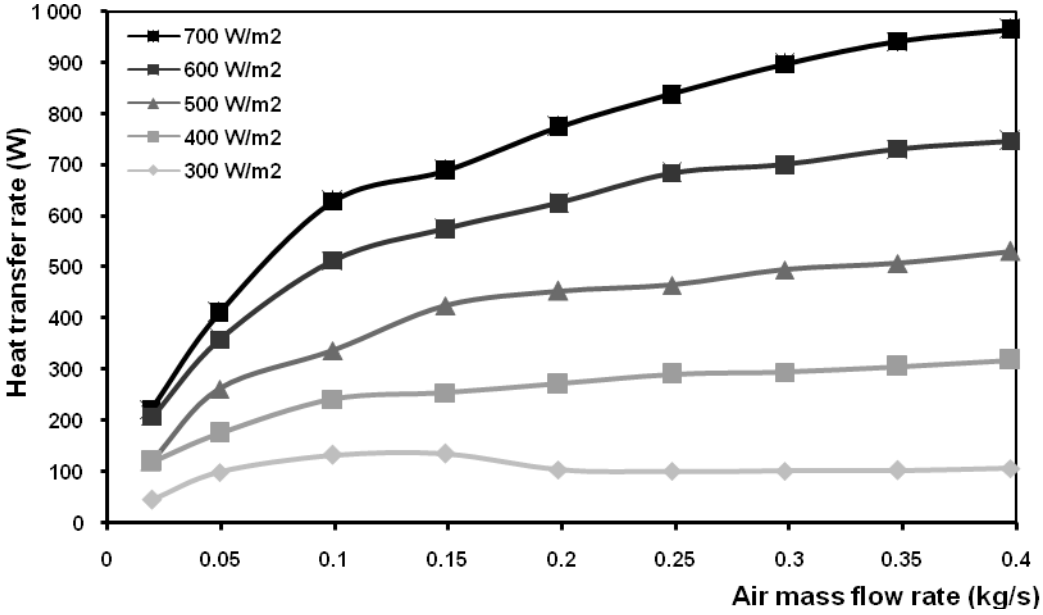

Fig. 14. Heat transfer rate to the air vs. mass flow rate for different perpendicular solar radiations (outdoor temperature: 10 ºC).

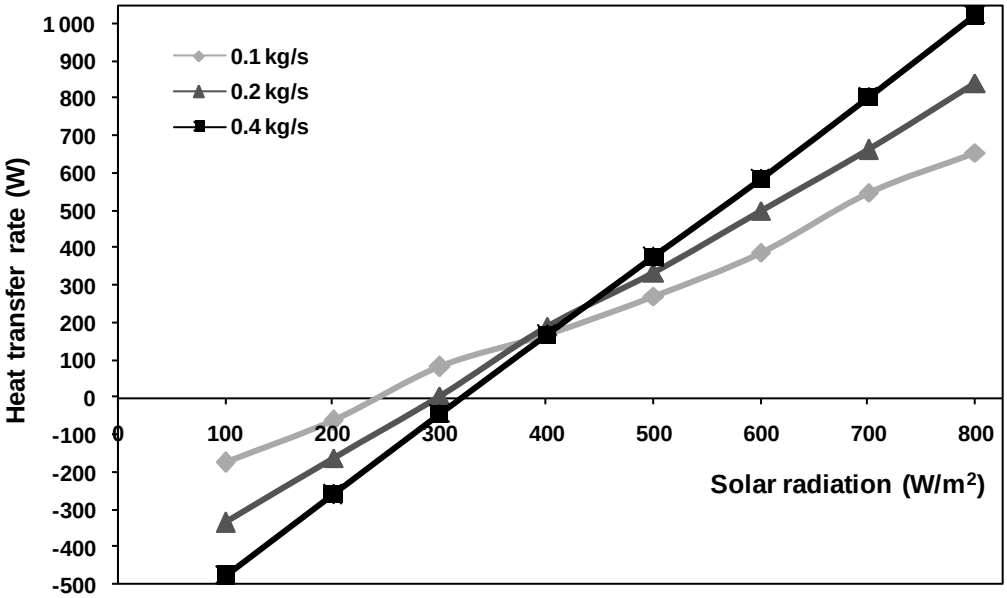

Fig. 15. Heat transfer rate to the air vs. perpendicular solar radiation for different air mass flow rates (outdoor temperature: 6 ºC).

Figure Captions

Fig. 1. Drawing of a traditional gallery.

Fig. 2. Photograph of demonstration container in northern Spain (South side). The gallery goes from the centre to the left.

Fig. 3. Interior of the glazed gallery.

Fig. 4. Cross-section of the gallery and the adjoining room.

Fig. 5. Operation of the gallery in winter (left) and summer (right) conditions.

Fig. 6. Geometry and boundary conditions. View from inside the room and along the gallery.

Fig. 7. Detail of the mesh at the inlet damper.

Fig. 8. Study of the turbulence model versus the number of cells.

Fig. 9. Temperature contours and velocity vectors in the middle cross-section.

Fig. 10. Stream lines coming out from the inlet louver.

Fig. 11. Temperatures on the vertical inner, top and bottom surfaces of the gallery.

Fig. 12. Thermograms of the exterior and interior of the gallery (perpendicular solar radiation 380 W/m^2, exterior temperature 16 ºC).

Fig. 13. Heat transfer rate to the air flow vs. perpendicular solar radiation, for different exterior temperatures (nominal mass flow rate 0.2 kg/s).

Fig. 14. Heat transfer rate to the air vs. mass flow rate for different perpendicular solar radiations (outdoor temperature: 10 ºC).

Fig. 15. Heat transfer rate to the air vs. perpendicular solar radiation for different air mass flow rates (outdoor temperature: 6 ºC).

Figure 1

Click here to download high resolution image

Figure 2

Click here to download high resolution image

Figure 3

Click here to download high resolution image

Figure 4

Click here to download high resolution image

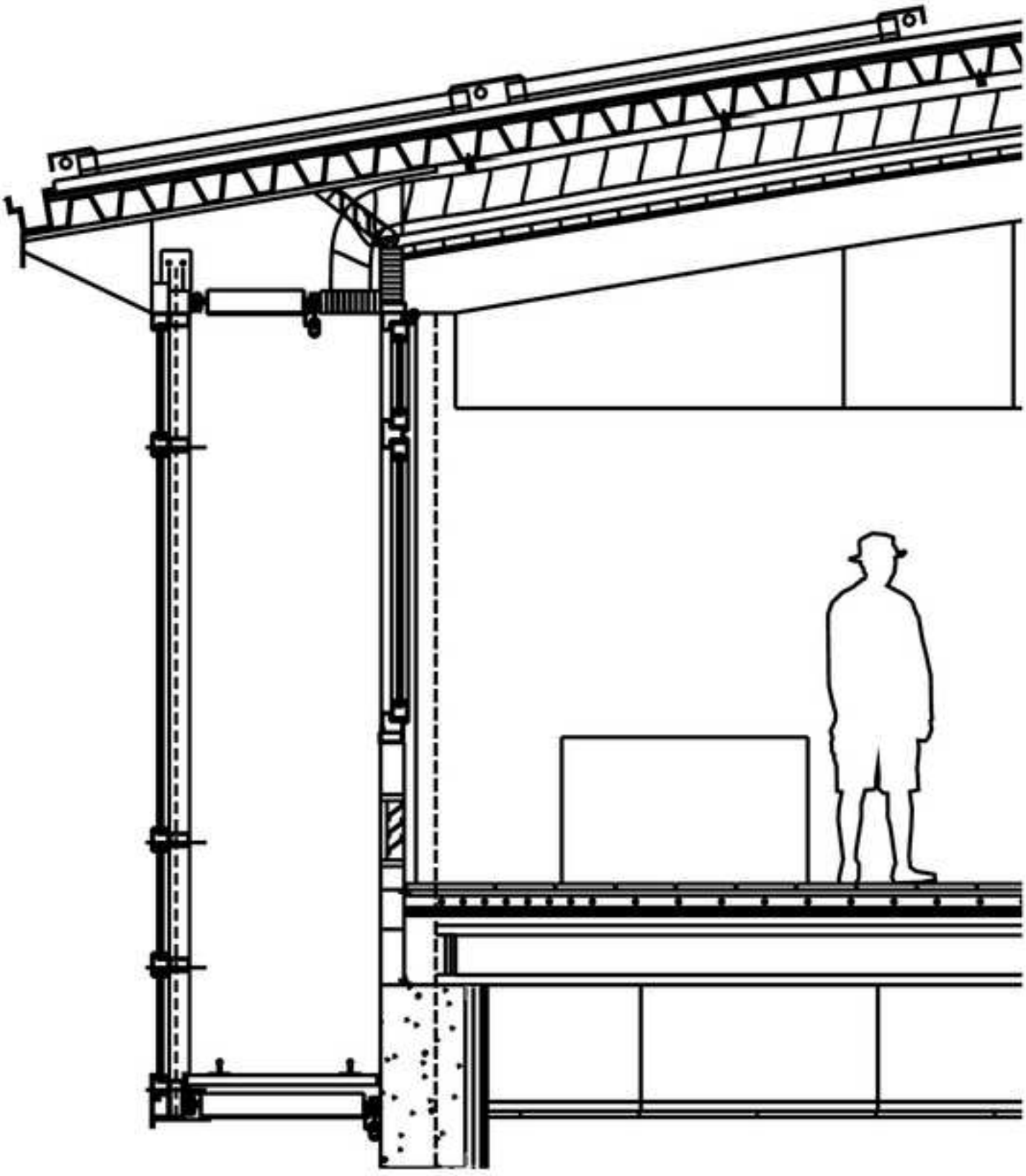

Figure 5

Click here to download high resolution image

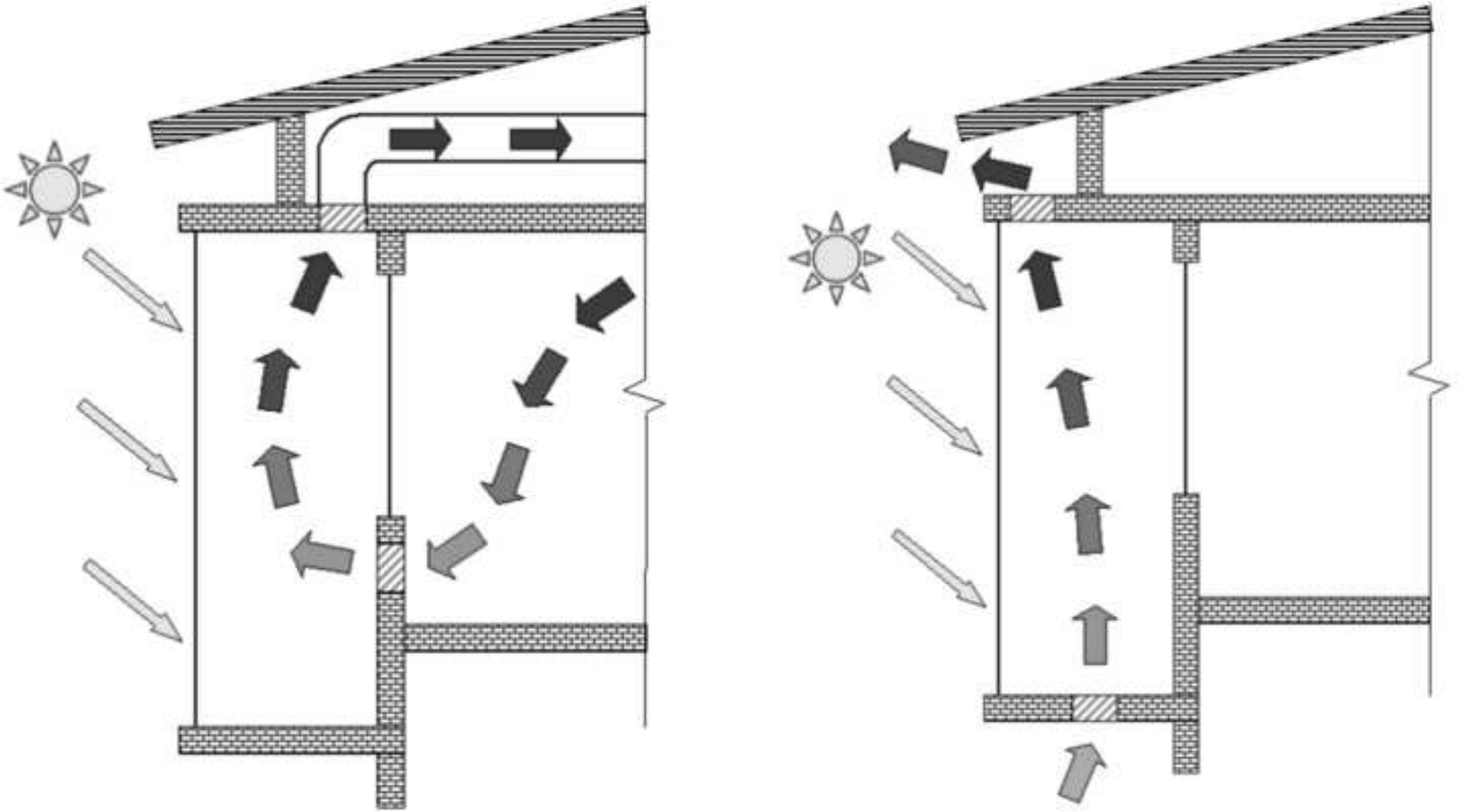

Figure 6

Click here to download high resolution image

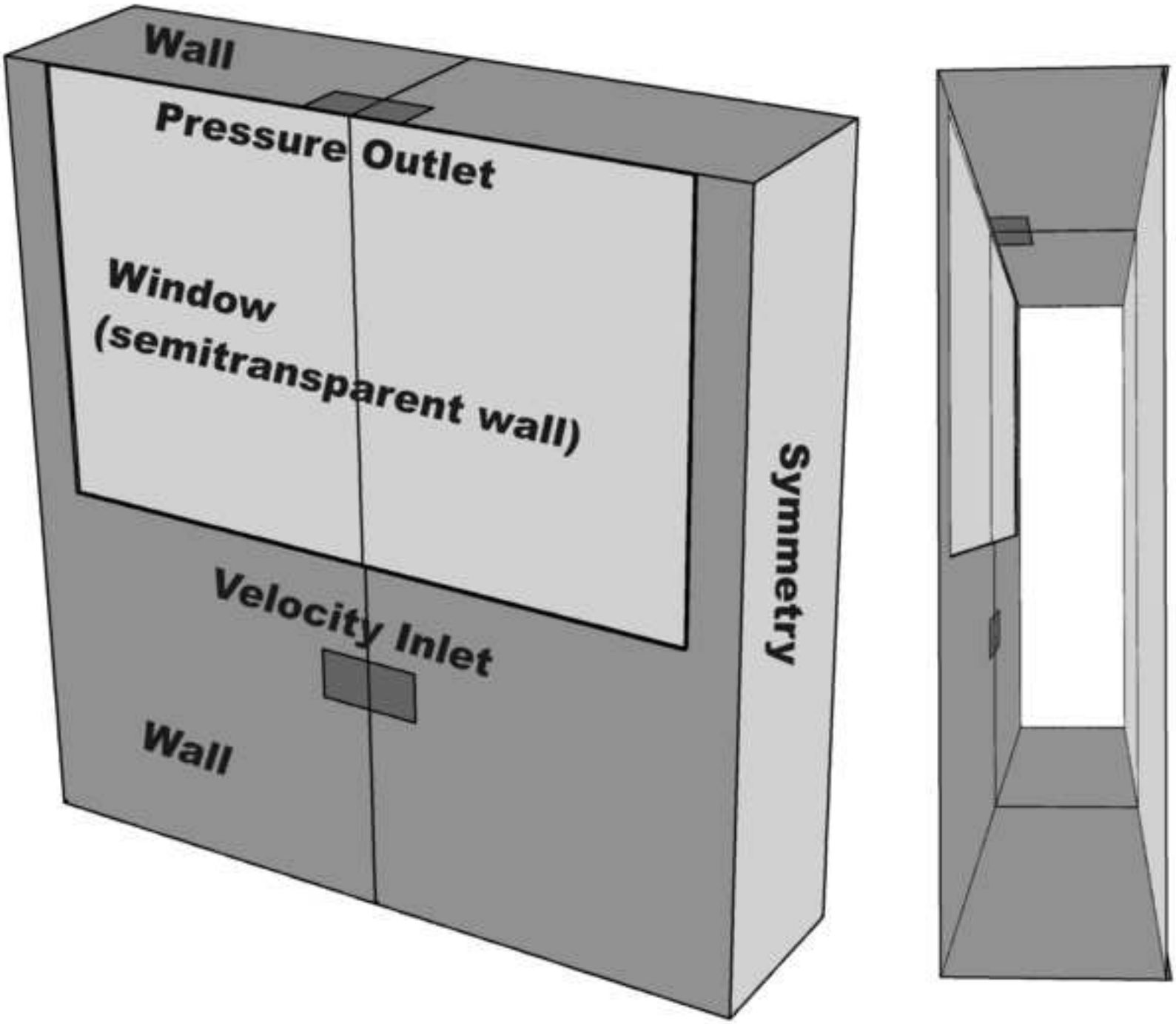

Figure 7

Click here to download high resolution image

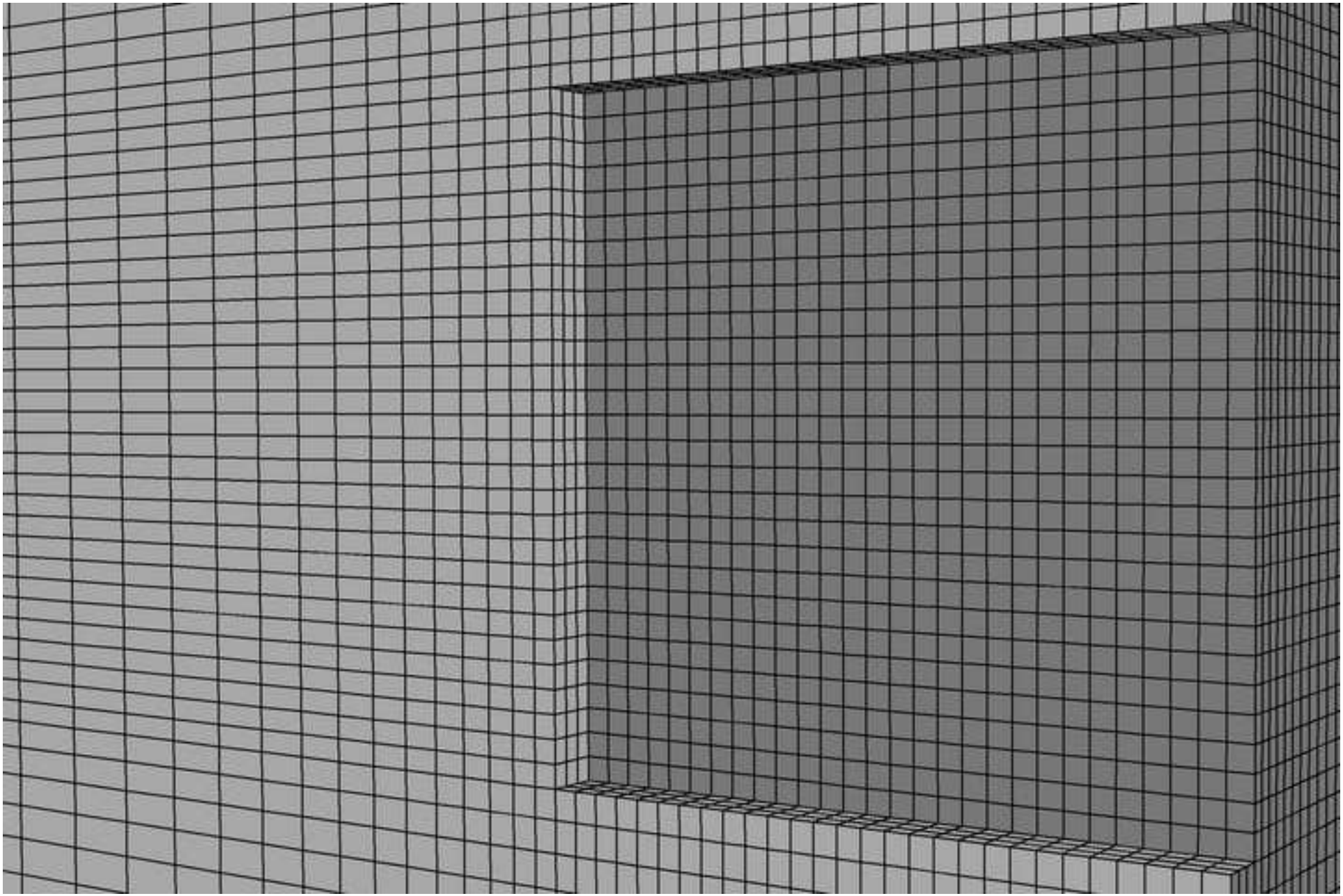

Figure 8

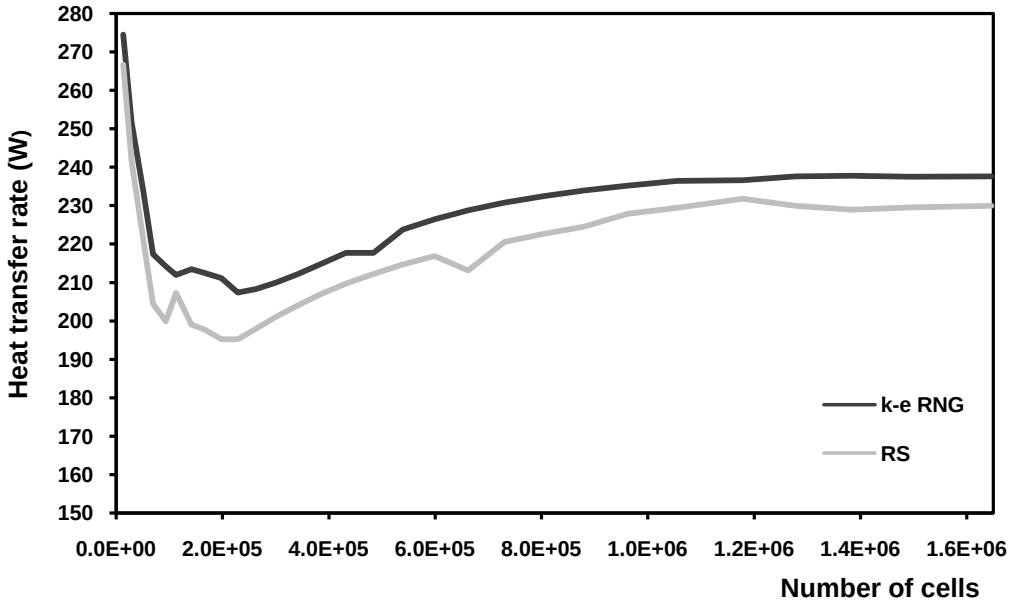
Heat transfer rate (W)
280
270
260
250
240
230
220
210
200
190
180
170
160
150
0.0E+00
2.0E+05
4.0E+05
6.0E+05
8.0E+05
1.0E+06
1.2E+06
1.4E+06
1.6E+06
Number of cells
k-e RNG
RS

Figure 9

Click here to download high resolution image

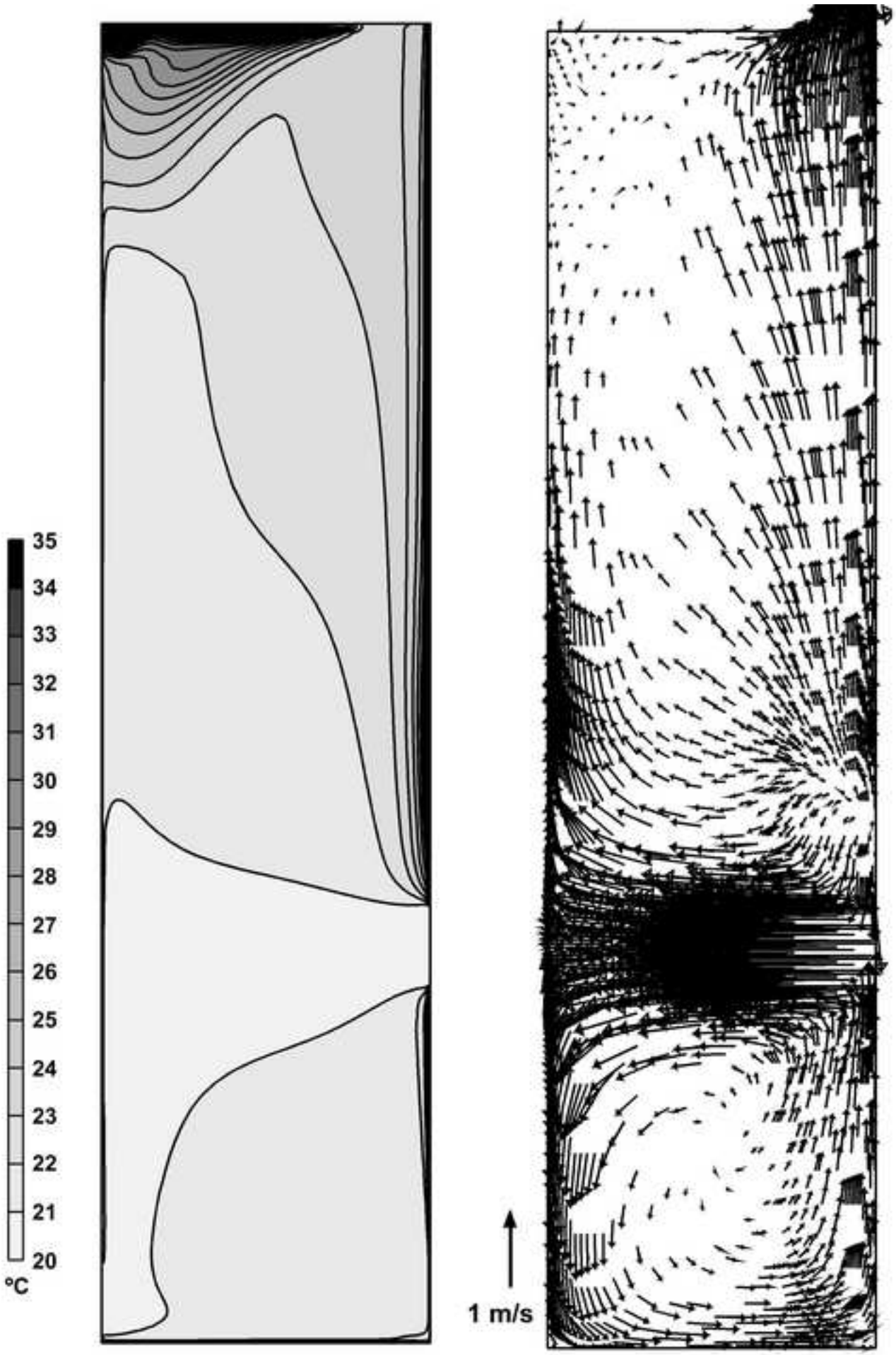

Figure 10

Click here to download high resolution image

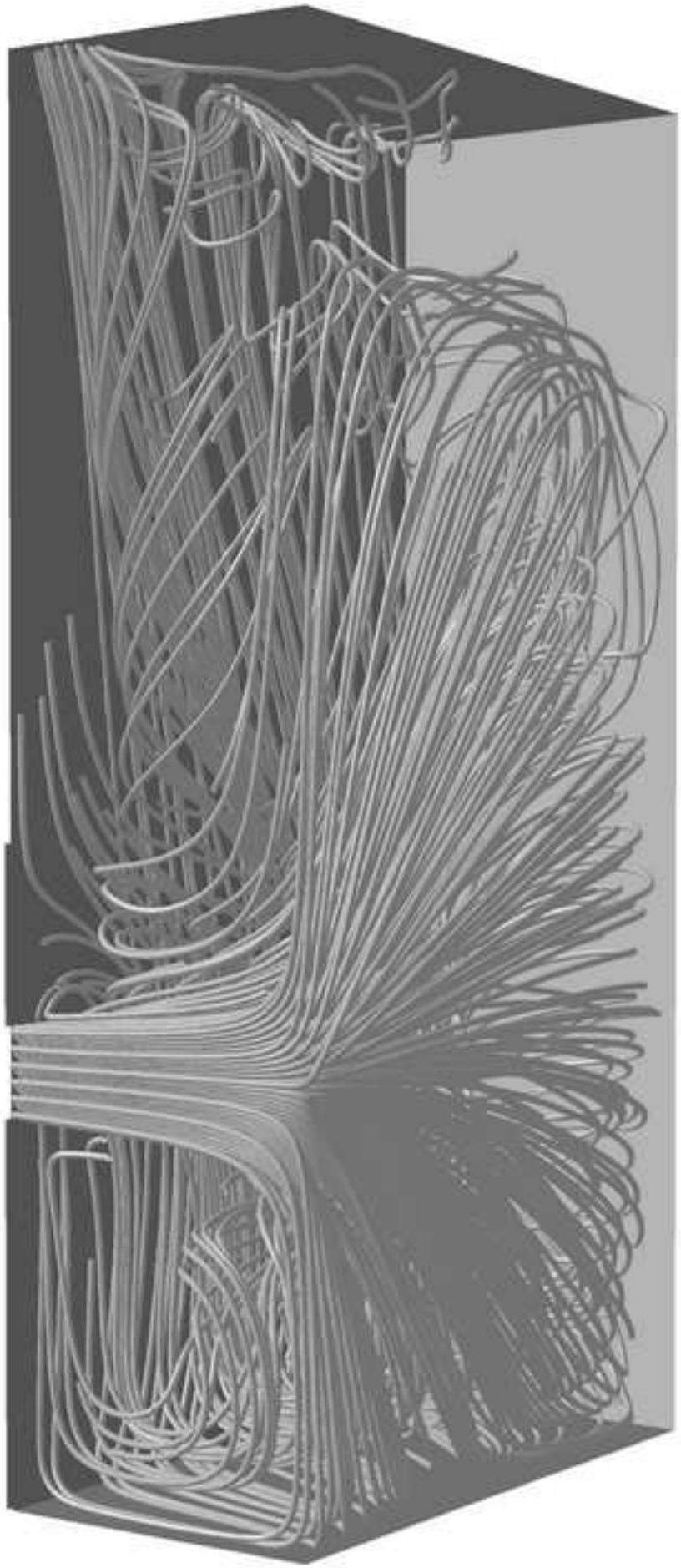

Figure 11

Click here to download high resolution image

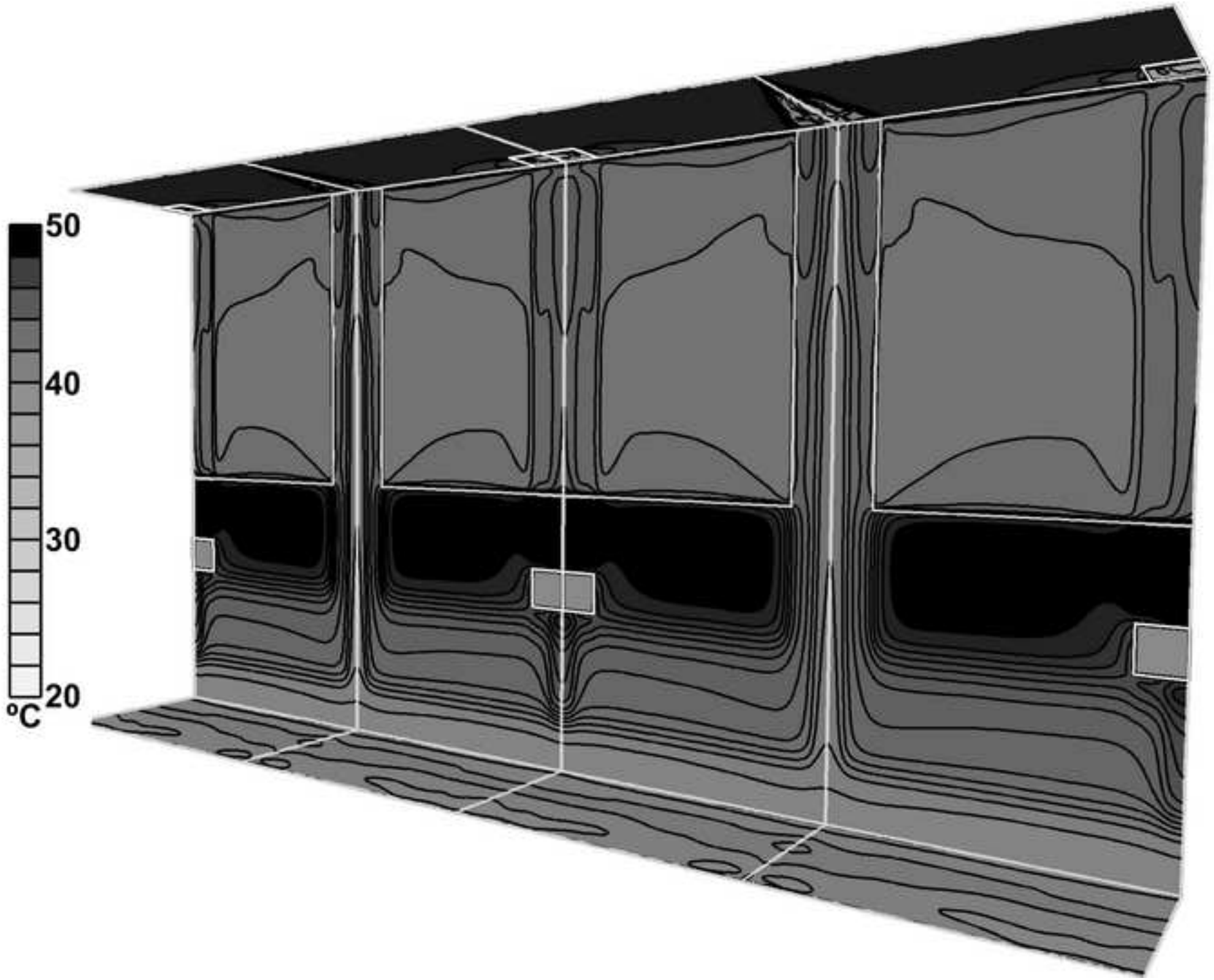

Figure 12

Click here to download high resolution image

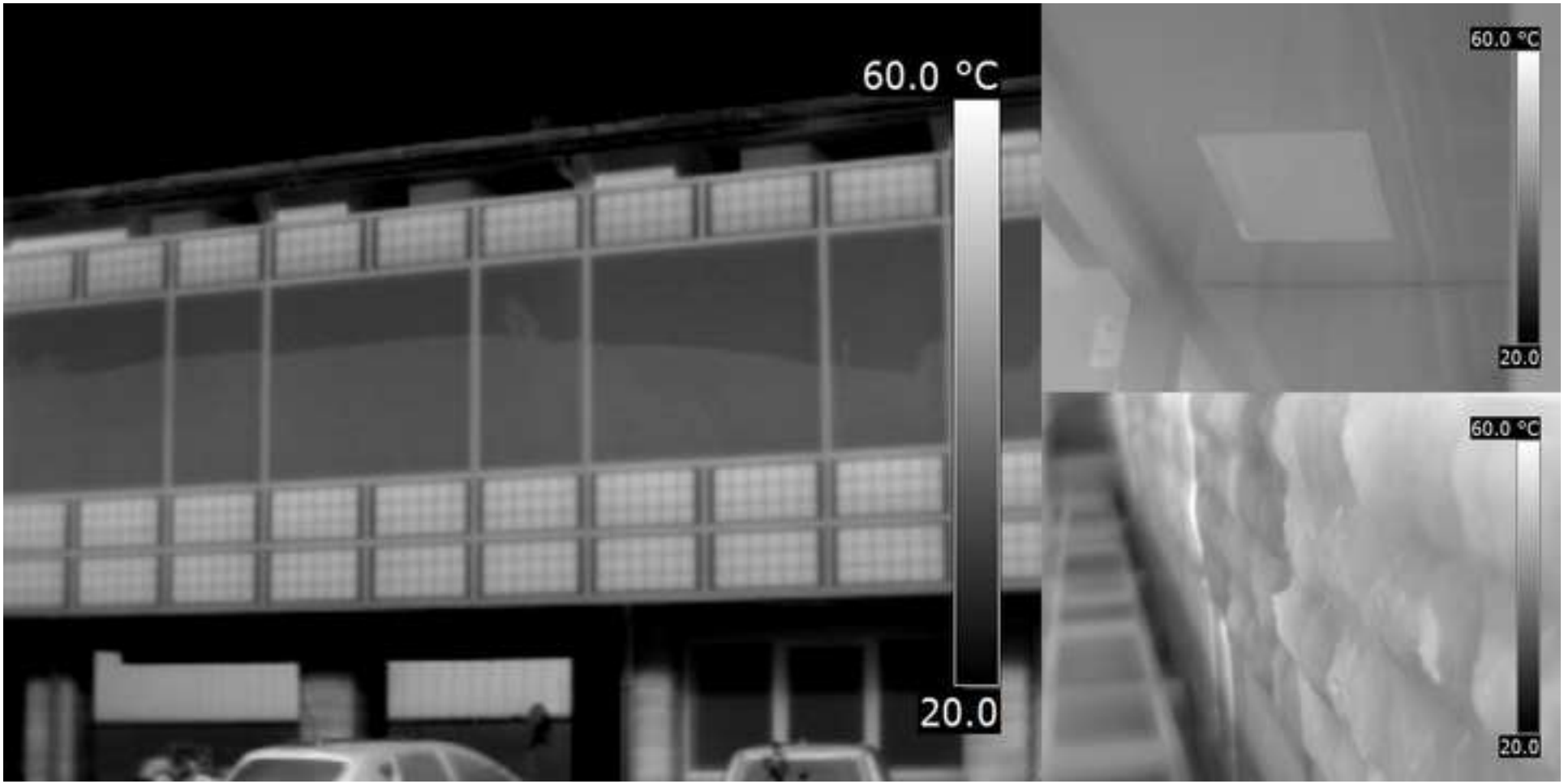

Figure 13

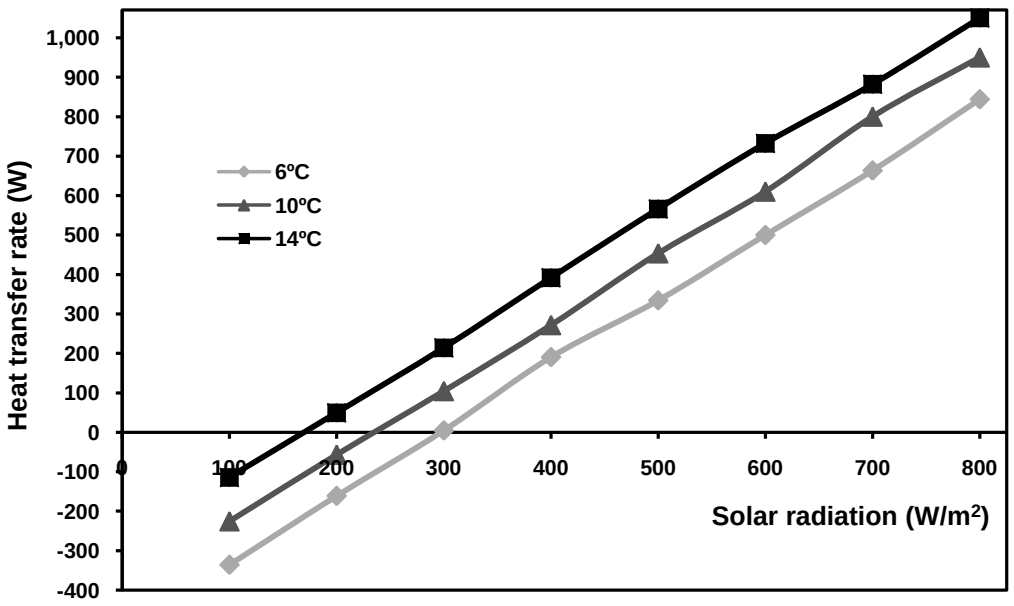
Heat transfer rate (W)
1,000
900
800
700
600
500
400
300
200
100
0
-100
-200
-300
-400
6ºC
10ºC
14ºC
0
100
200
300
400
500
600
700
800
Solar radiation (W/m2)

Figure 14

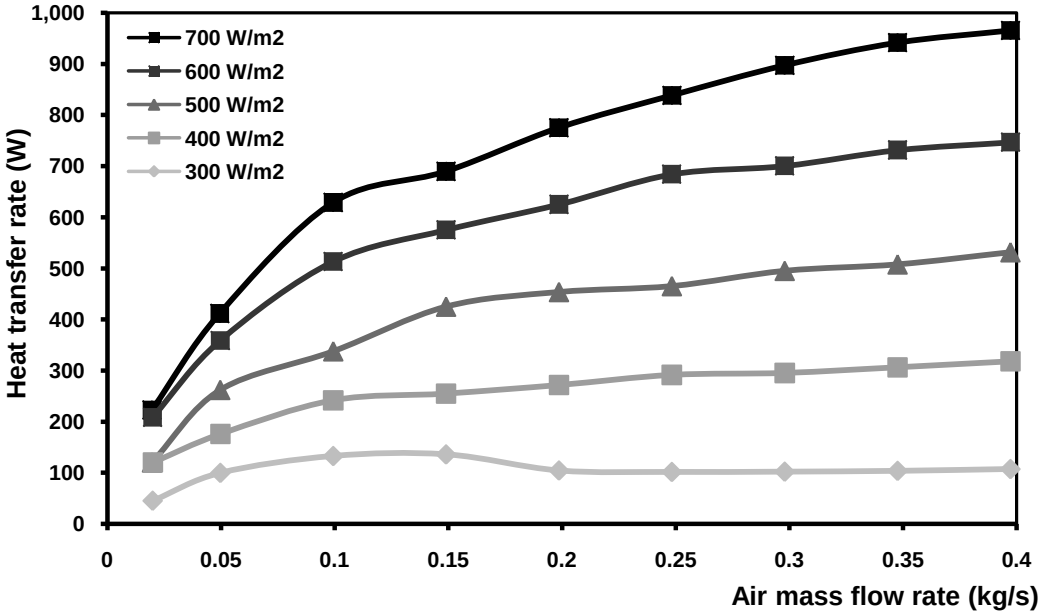
1,000
900
800
700
600
500
400
300
200
100
0
Heat transfer rate (W)
700 W/m2
600 W/m2
500 W/m2
400 W/m2
300 W/m2
0
0.05
0.1
0.15
0.2
0.25
0.3
0.35
0.4
Air mass flow rate (kg/s)

Figure 15

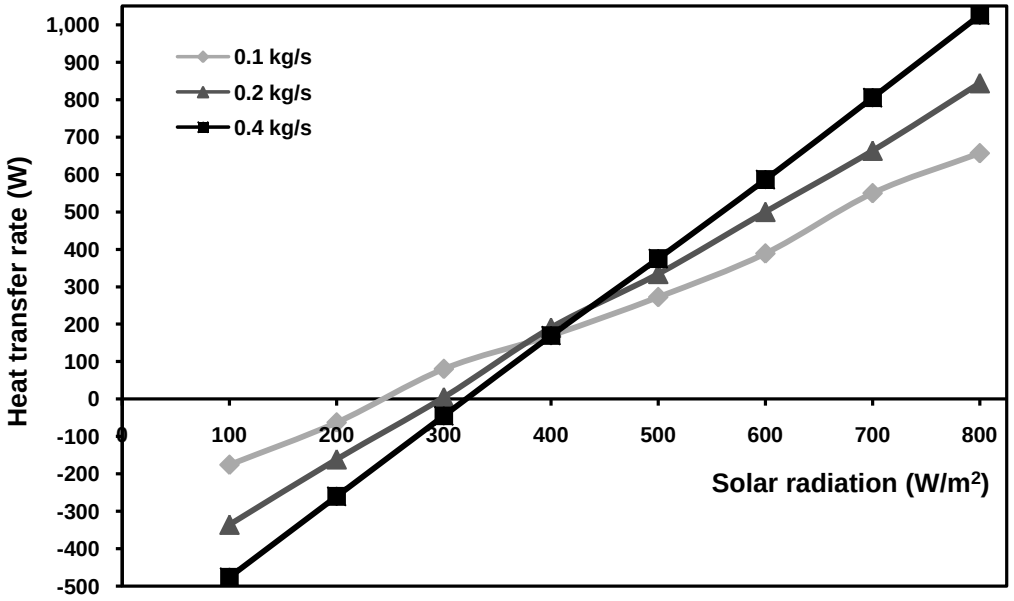
1,000
900
800
700
600
500
400
300
200
100
0
-100
-200
-300
-400
-500
0
100
200
300
400
500
600
700
800
0.1 kg/s
0.2 kg/s
0.4 kg/s
Heat transfer rate (W)
Solar radiation (W/m2)